Fatigue Crack Growth Behavior under Periodic Overload and Variable Amplitude Block Loading

Kentaro Yamada*, Naoki Okado** and Qiuliang Cao***

* Ph.D., Professor, Dept. of Civil Eng., Nagoya University, Furo-cho, Chikusa-ku, Nagoya 464-01
** M. of Eng., West Japan Railway Company, 4-24, Shibata 2-chome, Kita-ku, Osaka 530
*** Graduate Student, Dept. of Civil Eng., Nagoya University, Furo-cho, Chikusa-ku, Nagoya 464-01

Fatigue crack growth rates of structural steel SM520B were measured under periodic overload and variable amplitude block loading. For the former loading pattern, overload ratio and overload interval were selected as the parameters for the evaluation of fatigue crack growth retardation. It was found that higher overload ratio or larger overload interval caused larger retardation effect. For the latter one, effect of block size was investigated. Larger retardation effect was observed for larger block size.

Key words: periodic overload, variable amplitude block loading, load interaction

1. Introduction

Increase in frequent heavy trucks in recent years makes it necessary to re-assess fatigue durability of highway bridges[1]. In the fatigue assessment of such highway bridges, fatigue strength of the bridge components in long life region becomes a matter of increasing concern. It is because the stress spectra of highway bridge components usually fall into this region. However, it is known that the using of the traditional design approach, i.e., Miner's rule or equivalent stress range approach[2], often results in a too conservative estimation of fatigue life. One reason is that they neglect the effect of loading spectrum on the fatigue life prediction. The other reason is that they exclude the load interaction effect that may exist in the long life region. Therefore, a new prediction approach, in which the load interaction effect can be taken into account, is essential for more accurate fatigue assessment.

In the past two decades, many tests, including fatigue tests of weldments and fatigue crack growth rate measurements, were carried out in order to observe the load interaction effects on fatigue crack growth. For example, Abtahi and Albrecht in 1976[3] carried out fatigue tests on non-load carrying fillet welded joints to examine load interaction effects resulting from periodic overloads. The same specimens were used by Albrecht and Yamada in 1979[4] to study the variable amplitude block loading effects. Klippstein's tests in 1990[5] showed the effect of the shape of loading spectrum on fatigue crack growth. Load interaction effects were found in all of these tests. Such load interaction effects were partly explained by Elber's crack closure model[6] proposed in 1970s. It is referred as the plasticity-induced crack closure, according to which the premature contact may occur between crack surfaces even during the tensile portion of a stress cycle because of the residual plastic deformation in the wake of the growing crack. Based upon the crack closure concept, several computation models have been established, such as those proposed by Newman[7] and de Koning[8], both of which employed the Dugdale strip yield model[9] for calculating the crack-tip plasticity. The airplane industry tried a lot to apply this model to predict the fatigue lives of airplane parts and bodies. Some work has also been done in order to check their applicability to structural steels. However, there still remains much work to do in order to achieve a relatively accurate prediction on the fatigue lives of bridge components, which usually work at low stress range level and long fatigue life region.

The present study is among a series of experimental studies[10), 11)] aiming at establishing such kind of prediction approach. The loading spectra employed in these tests include single overload (SOL), periodic overload (POL), variable amplitude block loading (BL) and variable amplitude (VA) loading. The results of SOL tests have been reported elsewhere[12), 13)]. The present paper summarizes the achievements obtained through POL and BL tests.

In order to investigate the load interaction effect produced by POL or BL loading on welded bridge details, some measurements[3), 4)] were performed in the past two decades. The effects of various loading variables were discussed based on the measured fatigue lives. The current tests attempted to further understand the load interaction effect under POL and BL loading, for which fatigue crack growth rate measurements were carried out on center-cracked tension (CCT) specimens made of structural steel SM520B. In POL tests, overload ratio R_{OL}, i.e., the ratio of overload σ_{OL} to maximum load σ_{max}, and overload interval N_b, i.e., number of loading cycles between two successive overloads, were selected as the parameters in order to investigate the fatigue crack growth behavior. In BL tests, block size N_s, i.e., number of loading cycles in a loading block, was chosen as the parameter.

Table 1 POL loading condition

	$\Delta\sigma$ (MPa)	σ_{max} (MPa)	σ_{min} (MPa)	R_{OL}	σ_{OL} (MPa)	N_b	$\Delta\sigma_{eq}$ (MPa)
POLL-E2	70	90	20	1.4	126	100	70.572
POLL-E3						1,000	70.058
POLL-E4						10,000	70.006
POLH-E3	70	90	20	2.0	180	1,000	70.254
POLH-E4						10,000	70.026
POLH-5E4						50,000	70.005

Table 2 BL loading condition

Load No.	1	2	3	4	5	6	7	8	9	10
Relative Cycle Number (%)	1.7	22.3	10.8	3.1	4.7	30.6	15.9	1.6	2.1	7.2
$\Delta\sigma$ (MPa)	100.5	62.5	73.4	89.7	84.2	57.1	67.9	106.0	95.1	78.8
σ_{max} (MPa)	120.5	82.5	93.4	109.7	104.2	77.1	87.9	126.0	115.1	98.8
σ_{min} (MPa)	20	20	20	20	20	20	20	20	20	20

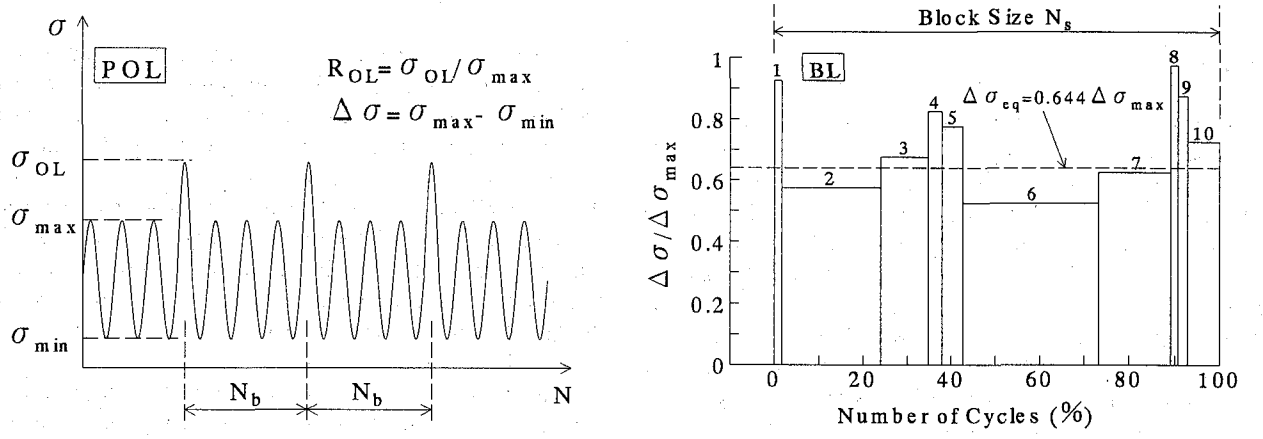

(a) Periodic overload

(b) Variable amplitude block loading

Fig. 1 Loading patterns

Normally load interaction effect results from high-low or low-high load sequences. The former may lead to fatigue crack growth retardation while the latter may lead to acceleration. In the present study, both effects were observed. In an extreme case where the overload ratio R_{OL} was high and the crack size a was small, crack arrest even took place.

2. Experiments

2.1 Test Specimens

Fatigue crack growth measurements were carried out on CCT specimens (t=10mm) made of SM520B steel. Both the material properties and the specimen features, including shape, dimension and surface processing method in the present tests were the same as those in SOL tests described in Refs. 12) and 13).

2.2 Loading Patterns

The POL and BL loading patterns used in the tests are schematically shown in Fig. 1. The detailed loading conditions are summarized in Tables 1 and 2.

For POL Loading, fatigue tests were carried out under two R_{OL} levels, i.e., R_{OL}=1.4 and 2.0. The former case included three tests named POLL-E2, POLL-E3 and POLL-E4, corresponding to N_b values of 100, 1,000 and 10,000, respectively. The latter case included three tests named POLH-E3, POLH-E4 and POLH-5E4, corresponding to N_b values of 1,000, 10,000 and 50,000, respectively. The equivalent stress range $\Delta\sigma_{eq}$, as shown in Table 1, is calculated by Eq.1.

$$\Delta\sigma_{eq} = \sqrt[m]{\frac{\sum(\Delta\sigma_i)^m \cdot n_i}{\sum n_i}} \quad (1)$$

Table 3 Specimen arrangement

Spec. No.	Test	Starting ΔK ($MPa\sqrt{m}$)	Ending ΔK ($MPa\sqrt{m}$)
1	POLL-E2	11.2	14.2
	POLL-E3	14.2	18.1
	POLL-E4	18.1	22.9
	POLL-E2	22.9	29.1
	POLL-E3	29.1	36.9
	POLL-E4	36.9	46.9
2	POLH-5E4	13.6	16.3
	POLH-E4	16.3	19.5
	POLH-E3	19.5	23.3
	POLH-5E4	23.3	27.9
	POLH-E4	27.9	33.4
	POLH-E3	33.4	40.0
3	BL-E4	11.2	13.9
	BL-E3	13.9	17.1
	BL-E2	17.1	21.2
	BL-E4	21.2	26.2
	BL-E3	26.2	32.4
	BL-E2	32.4	40.0
4	BL-E5	11.2	23.3

where $\Delta\sigma_i$ is the ith stress range, n_i is the corresponding number of cycles, and m is the slope of fatigue crack growth rate equation in log-log scale. In the present study, m is taken as 3.0.

The loading spectrum used in BL tests was the same as that described in Ref. 4), which was derived from stress histograms measured in short-span highway bridges in the U.S.A. in 1970s. One loading block of N_s cycles contained 10 bars corresponding to different loading levels. The block size N_s in the tests were selected as 100, 1,000, 10,000 and 100,000, corresponding to the four tests named BL-E2, BL-E3, BL-E4 and BL-E5, respectively.

2.3 Experimental Procedure

The experimental procedure was almost the same as that in the previous tests for SOL, except that the measurement intervals were decided according to the POL and BL loading spectra. In general, the measurement intervals ranged from 1,000 to 10,000, corresponding to different fatigue crack growth rates, i.e., small intervals for high rates and large intervals for low rates. In addition, the following two criteria were used. (1) When N_b or N_s was small, the measurement interval was selected as N_b or N_s, or its factored number to observe average fatigue crack growth rates in N_b or N_s. (2) For BL-E5, the measurement interval was decided based on the width of each bar in the loading block to obtain fatigue crack growth increment in each bar, if possible.

The test consisted of 4 specimens. To shorten the testing time, each specimen was used for several loading patterns. The stress intensity factor ranges ΔK at the starting and ending points of each loading pattern are listed in Table 3. Through this arrangement, the test data of each loading pattern in both the high-ΔK and low-ΔK regions can be obtained.

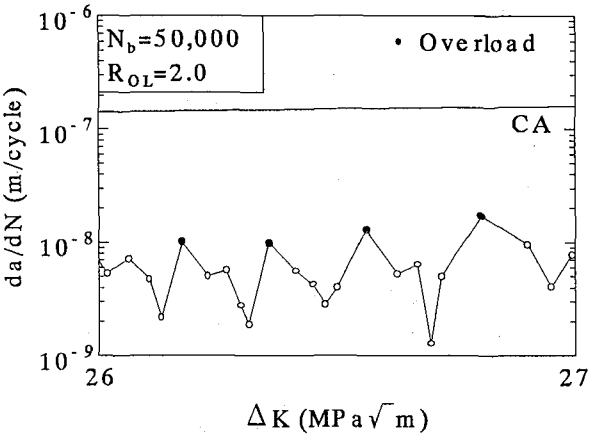

Fig. 2 Fatigue crack growth retardation of POLH-5E4

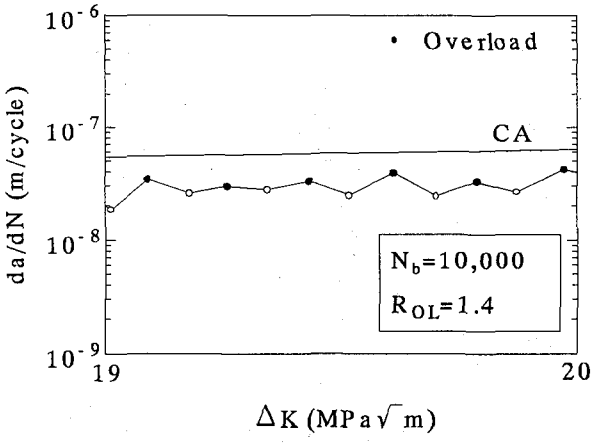

Fig. 3 Fatigue crack growth retardation of POLL-E4

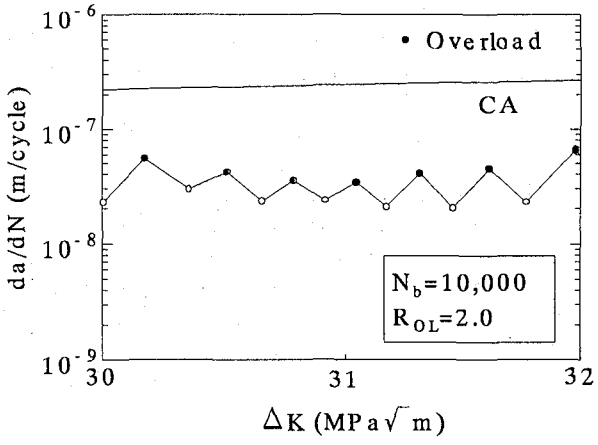

Fig. 4 Fatigue crack growth retardation of POLH-E4

3. Results of POL Tests

3.1 Fatigue Crack Growth Retardation

The fatigue crack growth rates, *da/dN*, of POLH-5E4 at ΔK ranging from 26 to 27 $MPa\sqrt{m}$ are shown in Fig. 2, along with the result of constant amplitude (CA) test in

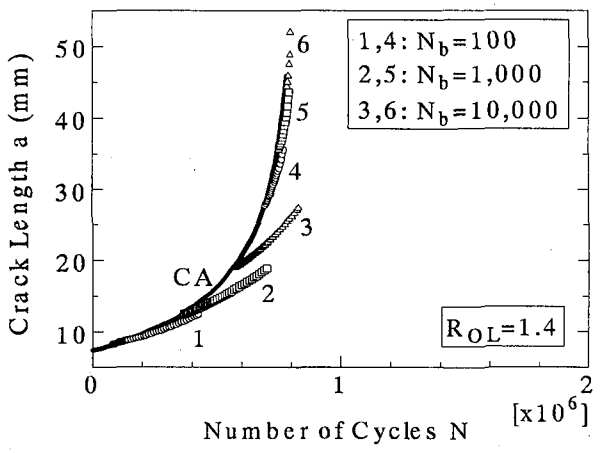

Fig. 5 Fatigue crack growth behavior in POLL tests

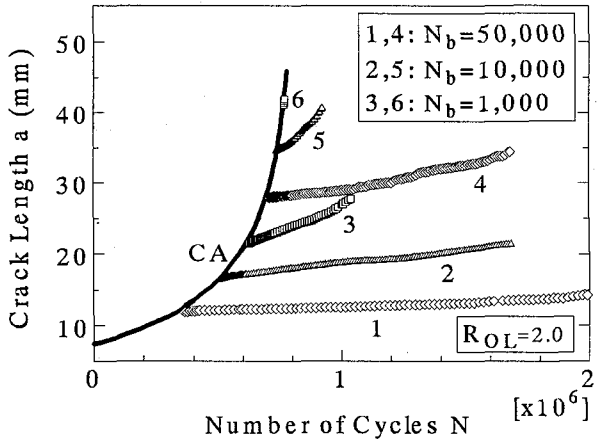

Fig. 6 Fatigue crack growth behavior in POLH tests

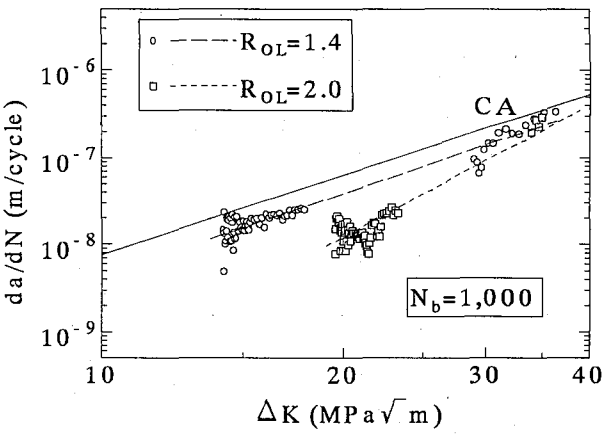

(a) Low overload interval N_b

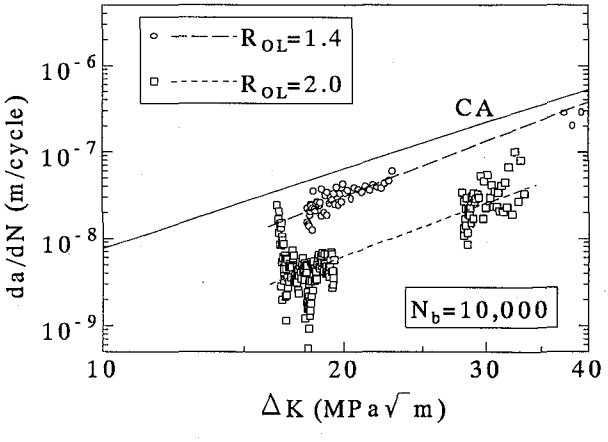

(b) High overload interval N_b

Fig. 7 Effect of overload ratio R_{OL}

which σ_{min} =20MPa and σ_{max} =90MPa. The measurement interval here is 10,000, one-fifth of the N_b=50,000. Therefore there are altogether 5 points for one loading block, each of which is an average value under 10,000 loading cycles. The solid symbol contains the overload.

The average *da/dN* with the overload is the highest, and then it gradually decreases. This indicates the fatigue crack growth retardation due to the overload, as in the case of SOL. However, for SOL case, fatigue crack growth rates increase gradually after they reach the lowest point, and finally recover to the level corresponding to CA loading. The process zone is called overload affected zone[14]. For POL case, the current retardation process is interrupted by the subsequent overload, since the overload interval is smaller than the overload affected zone. This makes the average *da/dN* hardly recover to that of CA loading. It fluctuates around a certain value below the CA level, as shown in Fig. 2.

Similarly, average *da/dN* of POLL-E4 and POLH-E4 at ΔK ranging from 19 to 20 MPa$\sqrt{m}$ and from 30 to 32 MPa$\sqrt{m}$, respectively, are shown in Figs. 3 and 4. The measurement intervals in these two regions are 5,000, half of the N_b=10,000. The solid symbols contain the overloads. When the overload ratio, R_{OL}, is 1.4, the average *da/dN* seems closer to that of CA, compared with the case of R_{OL}=2.0, as shown in Figs. 2 to 4. It implies that the smaller overload ratio causes less retardation effects.

In the other tests under smaller N_b, fatigue crack growth retardation effects are also found, i.e., average *da/dN* is lower than that of CA test. However, because measurement intervals in these tests are larger than the overload affected zones, the above-stated *da/dN* variations in a loading block are not available.

In the following discussion, the crack growth behavior, i.e., *a* versus *N* relationship, and the average *da/dN*, are plotted.

3.2 Fatigue Crack Growth Behavior, *a* versus *N*

Figures 5 and 6 show fatigue crack growth behavior, *a* versus *N*, under POLL and POLH loading. The data shown here are shifted either to left or right to coincide the starting point of each group of POL test data with the CA curve for easy comparison.

In Fig. 5, curves 1 to 6 correspond to the tests on specimen 1 under R_{OL}=1.4. It can be noticed that in each test, POL leads to fatigue crack growth retardation, which makes the fatigue crack growth rates slow down and *a* versus N curve deviate from that of CA. Moreover, in small crack

Table 4 Loading conditions when crack is near arrest

Starting a (mm)	Ending a (mm)	Loading Type	Loading Condition				ΔN	Δa (mm)
			σ_{max} (MPa)	σ_{min} (MPa)	R_{OL}	N_b		
8.000	8.395	CA	90	20	-	-	42,072	
8.395	8.411	POLH-5E4	90	20	2.0	50,000	150,002	+0.016
8.411	8.738	CA	180	20	-	-	1,617	+0.327
8.738	8.762	POLH-5E4	90	20	2.0	50,000	150,011	+0.024
8.762	9.365	CA	180	20	-	-	1,502	+0.603
9.365	9.323	POLH-5E4	90	20	2.0	50,000	150,004	-0.042
9.323	9.998	CA	180	20	-	-	2,698	+0.675
9.998	10.012	POLH-5E4	90	20	2.0	50,000	150,385	+0.014
10.012	10.604	CA	180	20	-	-	3,002	+0.628
10.604	10.647	POLH-5E4	90	20	2.0	50,000	210,010	+0.043
10.647	11.400	CA	180	20	-	-	4,104	+0.753

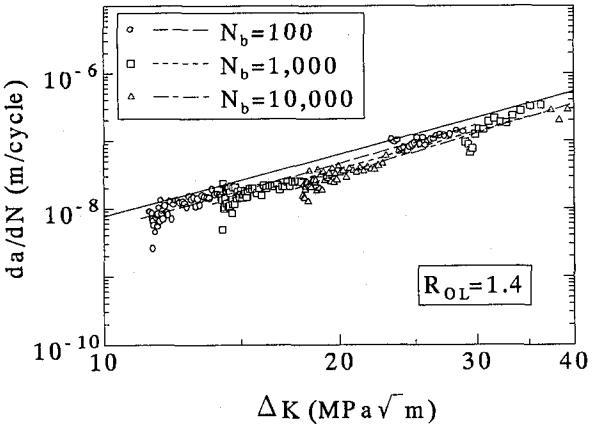

(a) Low overload ratio R_{OL}

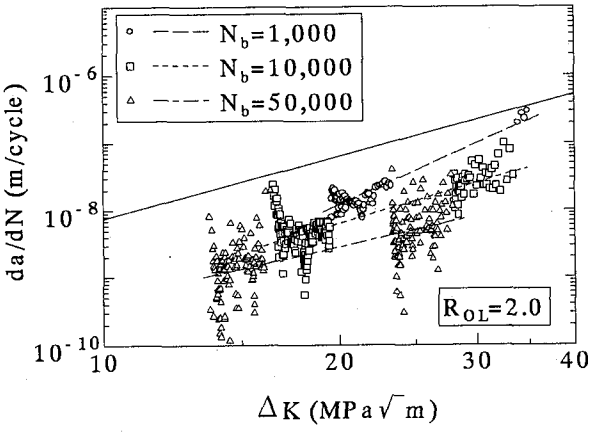

(b) High overload ratio R_{OL}

Fig. 8 Effect of overload interval N_b

region, i.e., in low-ΔK region, fatigue crack growth retardation increases with overload interval N_b. In high-ΔK region, however, this tendency becomes not clear. The a versus N curves in all tests approach to that of CA so that the differences among them tend to be small.

Figure 6 shows the a versus N relationships obtained under R_{OL}=2.0. The same phenomenon as described above is observed in both low-ΔK and high-ΔK regions. The fatigue crack growth retardation effect increases with overload interval N_b. Furthermore, the comparison between Figs. 6 and 5 shows that increasing overload ratio R_{OL} also leads to the increase in retardation effect.

3.3 Fatigue Crack Growth Rates, *da/dN*

In the followings, the average *da/dN* against stress intensity factor range ΔK are plotted to study the effects of overload ratio R_{OL} and overload interval N_b on fatigue crack growth retardation.

(1) Effect of Overload Ratio R_{OL}

Figure 7 shows a comparison between high-R_{OL} (2.0) and low-R_{OL} (1.4) case. The test data are for N_b=1,000 and 10,000. The regression line of each group of test data is also plotted.

From the figures, the following three phenomena can be observed:

(a) The average crack growth rates in POL tests are always lower than those of CA test.

(b) The amount of *da/dN* reduction is affected by overload ratio R_{OL}. The larger the overload ratio R_{OL} is, the more the retardation effects are.

(c) The average crack growth rates *da/dN* of high-R_{OL} case vary in a wider range than that of low-R_{OL} case.

(2) Effect of Overload Interval N_b

Figure 8 shows a comparison between different overload intervals N_b. In the figure, (a) gives the comparison of N_b=100, 1,000 and 10,000 for low-R_{OL} (1.4) case, and (b) gives the comparison of N_b=1,000, 10,000 and 50,000 for high-R_{OL} (2.0) case. The regression line of each group of test data is also plotted. From the figure, the following two phenomena can be observed:

(a) Increase in N_b results in a reduction in fatigue crack growth rates. It implies that retardation effect increases with the increase of N_b. As shown in Fig. 8(a), the *da/dN* gradually decreases as N_b increases at R_{OL}=1.4. And the effect is much larger, when the larger R_{OL}=2.0 is applied, as shown in Fig. 8(b). The average *da/dN* for N_b=50,000 is about one-tenth of that of CA.

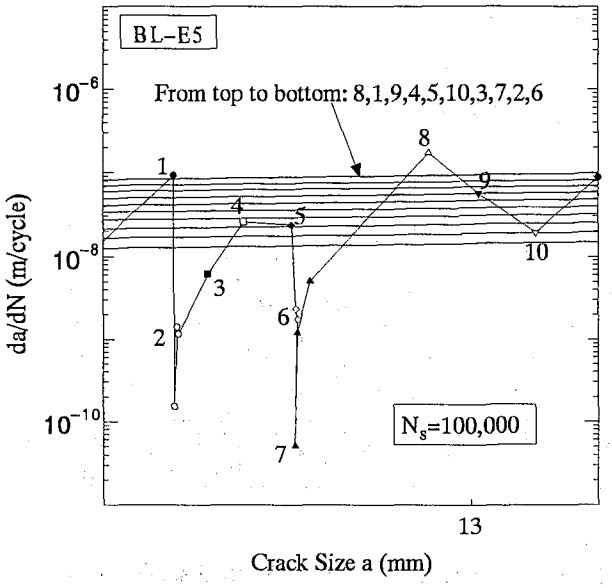

Fig. 9 Variation of *da/dN* in a loading block

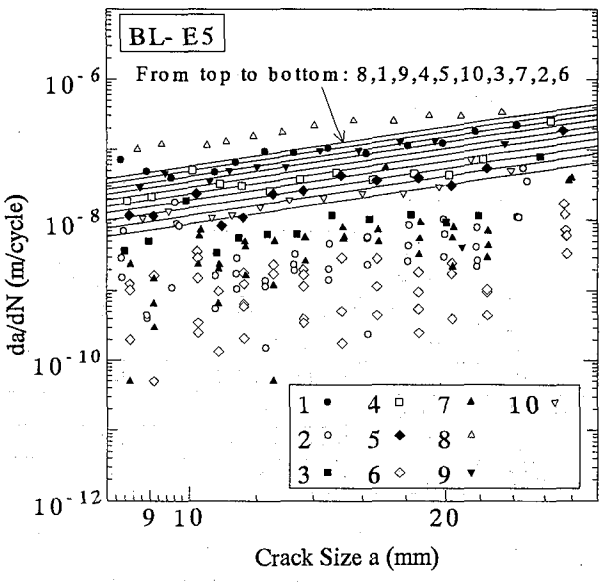

Fig. 10 Variation of da/dN

(b) The variation range of *da/dN* is normally wider for higher N_b. The reason may be that higher N_b causes *da/dN* to drop down to a lower value before the application of subsequent overload. This tendency is not so clear in the comparison between N_b=100 and 1,000 for R_{OL}=1.4, as shown in Fig. 8 (a). This may be because when R_{OL} is small, retardation is small, and the differences in *da/dN* for smaller N_b tend to be small.

3.4 Data in near Crack Arrest

In the present study, several crack arrests took place during the tests of R_{OL}=2.0 on specimen 2. Table 4 shows the loading conditions and corresponding crack sizes during this procedure. When POLH-5E4 loading was applied at a=8.395mm, very little crack growth increment was observed. Then, CA loading corresponding to the overload was applied to the specimen. The crack grew by 0.327mm. However, once POLH-5E4 was applied, crack grew very little again. Therefore, POLH-5E4 and CA were exerted alternatively on the specimen until the crack size reached 11.400mm, after which obvious crack growth increments could be observed under POLH-5E4 loading.

From the analysis of test data, it is known that increasing overload ratio R_{OL} or overload interval N_b leads to intensified effects of fatigue crack growth retardation. Crack arrest is an extreme case of crack retardation. It takes place under certain values of R_{OL} and N_b, for example, R_{OL}=2.0 and N_b=50,000 in the present test.

Crack arrest can be explained through the crack closure concept proposed by Elber[6]. When an overload is applied, it produces a large plastic zone ahead of the crack tip. These plastic deformation causes crack closure, which further decreases the fatigue crack growth rates by reducing the effective stress intensity factor range ΔK_{eff}. If plastic zone size is large enough, ΔK_{eff} approach a small value corresponding to threshold value of stress intensity factor range, ΔK_{th} [15], in the loading cycles following the overload. As a result, crack arrest occurs. In the case of multiple overloads, the crack propagates by the subsequent overload and a certain number of cycles following it. When a is large enough, for example 11.400mm in the present test, crack growth rates in measurable state can be observed and therefore crack arrest condition is overcome.

4. Results of BL Tests

4.1 Fatigue Crack Growth Retardation and Acceleration

Figure 9 shows *da/dN* versus a relationship in a loading block of BL-E5 at around 13mm. The CA crack growth rates corresponding to each loading level in the loading block are also plotted in the figure in the sequence of 8, 1, 9, 4, 5, 10, 3, 7, 2 and 6 from the top to the bottom. These CA results are obtained from a test with stress range of 70 MPa[13]. Crack growth rates of other stress ranges are calculated by Paris's equation expressed by Eq.2.

$$da/dN = C \cdot \left[F(a) \cdot \Delta\sigma \cdot \sqrt{\pi a} \right]^m \qquad (2)$$

where C and m are material constants and $F(a)$ is the crack size-related correction factor.

The crack growth retardation effects, which occur in loading level 2, 3, 6 and 7, can be seen from the figure. From the BL loading spectrum shown in Fig. 1 (b), it can be inferred that the retardation effects of loading levels 2 and 3 result from the precedent higher loading level 1, and those of loading levels 6 and 7 result from previous higher loading levels 4 and 5. On the other hand, loading level 8 shows that crack growth rate is higher than the corresponding CA line. The small acceleration effect is observed. This may be due to the effects of precedent lower loading levels 6 and 7.

Figure 10 shows all of the *da/dN* versus a data. The fatigue crack growth rates of 2, 3, 6 and 7 are lower than their corresponding CA levels, which indicates the occurrence of fatigue crack growth retardation. The fatigue crack growth rates of loading level 8 seem to be higher than

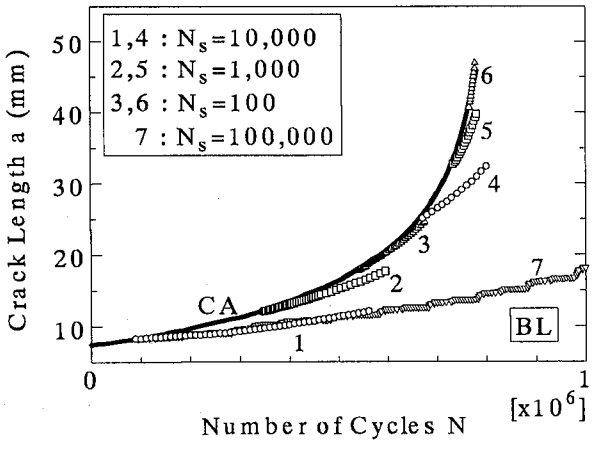

Fig. 11 Fatigue crack growth behavior in BL tests

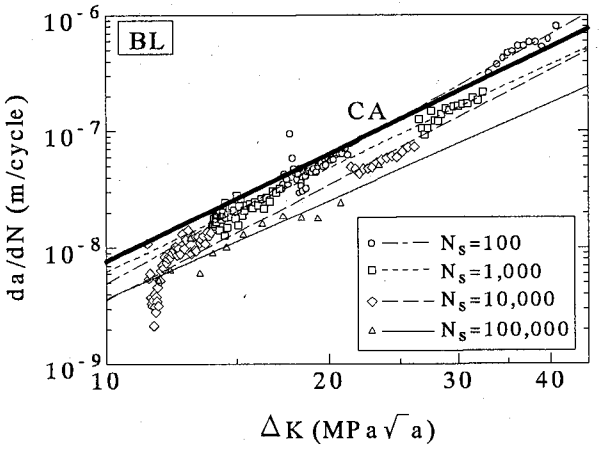

Fig. 12 Fatigue crack growth rates in BL tests

that of the corresponding CA level, which indicates the occurrence of fatigue crack growth acceleration.

4.2 Fatigue Crack Growth Behavior, *a* versus *N*

Figure 11 shows the a versus N relationships of BL tests along with that of CA test. For easy comparison, the starting point of each test is plotted at the corresponding CA curve by shifting the point either to left or right.

In the figure, fatigue crack growth retardation can be clearly found in most of the tests, although the equivalent stress range of BL loading is 68.26MPa that is almost same as the CA stress range. From the above discussion, the retardation effect in levels 2, 3, 6 and 7 seem to contribute to the overall retardation effects. The small acceleration effect of level 8 is overwhelmed because the number of cycles in level 8 is only 1.6 percent of N_s. The test of N_s=100 shows little effect of retardation in high-ΔK region. The crack growth rates of it almost coincide with that of CA data.

Increase in the block size N_s leads to larger deviation of the crack growth behavior from that of CA. It implies that the larger crack growth retardation effect is produced for the larger N_s. This is in the same tendency as that observed in BL fatigue tests on welded joints[4].

4.3 Fatigue Crack Growth Rates, *da/dN*

Figure 12 shows the *da/dN* versus ΔK relationships of all BL tests, the N_s values of which range from 100 to 100,000. For the test of N_s=100,000, the average *da/dN* in each loading block are given instead of showing all of the test data.

The *da/dN* of BL-E2 (N_s=100) are close to that of the CA test. With the increasing of N_s, the retardation effect becomes larger. Compared with the *da/dN* of CA loading, about one half of the *da/dN* is observed when N_s=100,000.

5. Conclusions

In the present study, fatigue crack growth rates of structural steel SM520B were measured under POL and BL loading conditions. The effects of overload ratio R_{OL} and overload interval N_b on crack growth behavior in POL tests, and the effects of block size N_s in BL tests were investigated based upon the test results. The main findings are summarized as follows:

1. Under the present loading conditions, crack growth retardation effects exist in both POL and BL tests, which makes the fatigue crack growth rates in these tests lower than those in CA tests. A small fatigue crack growth acceleration effect is also observed in a bar in low-high load sequence of BL loading.
2. Increase in overload interval N_b or increase in overload ratio R_{OL} leads to larger fatigue crack growth retardation effects in POL tests.
3. In the POL test of R_{OL}=2.0 and N_b=50,000, near crack arrest condition occurred when crack size was smaller than 11.5mm.
4. With the increasing in block size N_s in BL tests, the retardation effects tend to be larger and the variation range of crack growth rates becomes wider. The number of the precedent overload or underload cycles can provide the corresponding explanations.

Acknowledgement

This research is the part of the research on the fatigue life evaluation of welded members subjected to large number of small stress ranges in the long fatigue life region. It was jointly supported by the Grant-in-Aids of Ministry of Education, Science, Sports and Culture, and the research funds from Nagoya Expressway Authority and Kozai-kurabu. The authors thank to Professor A. Kondo of Meijyo University and Mr. S. Kainuma for their valuable discussion.

References

1) Subcommittee for Investigation of Fatigue Damage of Steel Structures, Committee for Steel Structures, *Survey of Fatigue Damages in Steel Bridges, Proc. of JSCE*, No. 368/I-5, April, 1986.
2) Japanese Society of Steel Construction, *Fatigue Design Recommendations for Steel Structures (English Version)*, December, 1995.
3) Abtahi, A. and Albrecht, P., Fatigue of periodically overloaded stiffener detail, *Proc. of ASCE, Journal of Structural Division*, Vol. 102, No. ST11, pp. 2103-2119, November, 1976.

4) Albrecht, P. and Yamada, K., Simulation of service fatigue loads for short-span highway bridges, *Service Fatigue Loads Monitoring, Simulation, and Analysis, ASTM STP 671*, Abelkis, P. R. and Potter, J. M., Eds., American Society for Testing and Materials, pp. 255-277, 1979.
5) Melhem, H. G. and Klippstein, K. H., A study on variable amplitude load fatigue: Work-in Progress, Research Report No. ST-6, *University of Pittsburgh*, January, 1990.
6) Elber, W., The significance of fatigue crack closure, *Damage Tolerance in Aircraft Structures, ASTM STP 486*, pp. 230-242, 1971.
7) Newman, J. C., Jr., A crack-closure model for predicting fatigue crack growth under aircraft spectrum loading, *Methods and Models for Predicting Fatigue Crack Growth under Random Loading, ASTM STP 748*, pp. 53-84, 1981.
8) de Koning, A. U. and Liefting, G., Analysis of crack opening behavior by application of a discretized strip yield model, *Mechanics of Fatigue Crack Closure, ASTM STP 982*, pp. 437-458, 1988.
9) Dugdale, D. S., Yielding of steel sheets containing slits, *Journal of Mechanics and Physics of Solids*, Vol. 8, pp. 100-104, 1960.
10) Cheng, X. H., Fatigue life evaluation of welded structural members under variable amplitude loadings, *Doctoral thesis, Nagoya University*, Nagoya, Japan, June, 1994.
11) Okado, N., Fatigue crack growth behavior of structural steel under periodic overload and variable amplitude loading, *Master thesis, Nagoya University*, Nagoya, Japan, March, 1997.
12) Cheng, X. H and Yamada, K., Fatigue crack growth rate measurement of structural steel under overload conditions, *Proc. of JSCE, Structural Eng./Earthquake Eng.*, Vol. 11, No. 1, pp. 45-52, April, 1994.
13) Yamada, K., Cao, Q. L., Okukara, Y. and Cheng, X. H., Fatigue crack growth behavior of various structural steel after single and periodic overload, *Nagoya University*, Nagoya, Japan, September, 1997, to be published.
14) Anderson, T. L., *Fracture Mechanics: Fundamentals and Applications, Second edition*, CRC Press, Boca Raton, pp. 534-536, 1995.
15) Schijve, J., Fatigue crack closure: observations technical significance, *Mechanics of Fatigue Crack Closure, ASTM STP 982*, Newman, J. C., Jr. and Elber, W., Eds., American Society for Testing and Materials, Philadelphia, pp. 5-34, 1988.

(Received September 26, 1997)